TECHNICAL NOTES

NATIONAL ADVISORY COMMITTEE FOR AERONAUTICS

No. 385

TESTS OF SIX SYMMETRICAL AIRFOILS IN THE VARIABLE DENSITY WIND TUNNEL

By Eastman N. Jacobs
Langley Memorial Aeronautical Laboratory

Washington
July, 1931

NATIONAL ADVISORY COMMITTEE FOR AERONAUTICS

TECHNICAL NOTE NO. 385.

TESTS OF SIX SYMMETRICAL AIRFOILS IN THE VARIABLE DENSITY WIND TUNNEL

By Eastman N. Jacobs

SUMMARY

This paper is the first of a series covering an investigation of a family of airfoils all formed from a basic profile. It gives in preliminary form the results obtained from tests in the N.A.C.A. variable density wind tunnel of six symmetrical airfoils, differing only in maximum thickness. The maximum thickness-to-chord ratios are 0.06, 0.09, 0.12, 0.15, 0.18, and 0.21. The results are analyzed with a view to indicating the variation of the aerodynamic characteristics with profile thickness.

INTRODUCTION

The forms of the airfoil sections that are in common use today are the result of a more or less systematic investigation made at Göttingen of a large number of airfoils. Previously airfoils such as the R.A.F. 15 and U.S.A. 27, developed from airfoil profiles investigated in England, were widely used. Because most airfoils have been developed from low-scale tests, the forms developed may not be the optimum for full-scale values of the Reynolds Number. A number of airfoils have been investigated in the variable density wind tunnel at values of the Reynolds Number approaching those of flight (reference 1), but with the exception of the M series and a series of propeller sections, the airfoils have not been related in such a way that the results could be satisfactorily correlated.

The object of an investigation now being carried out by the National Advisory Committee for Aeronautics is to obtain the characteristics, at large values of the Reynolds Number, of a wide variety of related airfoils. The bene-

fits of a systematic investigation of airfoil profiles at large values of the Reynolds Number are so self-evident that it is hardly necessary to point them out. Not only do the results of such investigations greatly facilitate the choice of the most satisfactory airfoil for a given application but, because the results may be correlated to indicate the trends of the aerodynamic characteristics with changes of shape, they may point the way to the design of new shapes having better characteristics.

Airfoil profiles may be considered as made up of certain profile thickness forms disposed about certain mean camber lines. The major shape variables then become two: the thickness form and the mean camber line form. The thickness is of particular importance from a structural standpoint. On the other hand, the form of the mean camber line determines almost independently some of the most important aerodynamic properties of the airfoil section, e.g., the pitching moment characteristics and the angle of zero lift.

The related airfoil profiles were obtained for this investigation by changing systematically these shape variables. A single basic thickness variation was chosen for the first group of airfoils. Sections having a different maximum thickness were obtained by the application of a factor to all the basic ordinates. The following ratios of maximum thickness-to-chord were chosen: 0.06, 0.09, 0.12, 0.15, 0.18, and 0.21. The cambered profiles were then obtained by combining these thickness forms with different mean camber lines. Since this report does not deal with the cambered airfoils, it will be sufficient to state that the various mean camber line forms are obtained by varying the maximum camber and by varying the distance from the leading edge to the position of the maximum camber. The airfoils so produced are designated by a number of four digits; the first indicates the maximum mean camber; the second, the position of the maximum mean camber; and the last two, the maximum thickness. Thus the N.A.C.A. 2315 airfoil has a maximum mean camber of 2 per cent of the chord at a position 0.3 of the chord from the leading edge, and a maximum thickness of 15 per cent of the chord; the N.A.C.A. 0012 is a symmetrical airfoil having a maximum thickness of 12 per cent of the chord.

This note presents in preliminary form the results of the tests of the first group of six airfoils. These tests

were made in April, 1931. Since these airfoils may be considered as the basic sections from which the others will be formed, the results are of particular importance. It is therefore considered desirable to present these results before the tests of all the airfoils of the series are completed and the results analyzed.

DESCRIPTION OF AIRFOILS

Well-known airfoils of a certain class, including the Göttingen 398 and the Clark Y, which have proved to be efficient, are nearly alike when their mean camber is removed and they are reduced to the same thickness. A thickness variation similar to that of these airfoils was therefore chosen for the development of the N.A.C.A. airfoils. A formula defining the shape was used as a method of producing fair profiles.

If the chord is taken along the x axis from 0 to 1, the ordinates y are given by a formula of the type

$$\pm y = a_0 \sqrt{x} + a_1 x + a_2 x^2 + a_3 x^3 + a_4 x^4.$$

The equation was adjusted to give the desired shape by imposing the following conditions to determine the constants:

1. Maximum ordinate 0.1 at 0.3 chord

$$y = 0.1 \text{ at } x = 0.3$$

$$\frac{dy}{dx} = 0 \text{ at } x = 0.3$$

2. Thickness of trailing edge

$$y = 0.002 \text{ at } x = 1$$

3. Trailing edge angle

$$\frac{dy}{dx} = -0.234 \text{ at } x = 1$$

4. Nose shape

$$y = 0.078 \text{ at } x = 0.1$$

The ordinates of the basic section, which is a symmetrical section having a total thickness of twenty per cent of the chord, are then given by the formula

$$\pm y = 0.296900\sqrt{x} - 0.126000x - 0.351600x^2 + 0.284300x^3 - 0.101500x^4$$

The curve of the basic section, shown in Figure 1, may be compared with the plotted points on the same figure that were obtained by removing the mean camber from the Göttingen 398 and the Clark Y sections, and applying a factor to the resulting thickness curves to bring them to the same maximum thickness.

The ordinates of the basic section as given by the formula are multiplied by a factor to obtain the related sections having any desired maximum thickness. The leading-edge radius for the basic section is found from the formula to be

$$r = \frac{a_0^2}{3}$$

or, for a derived section of maximum thickness-to-chord ratio t, the leading-edge radius expressed as a ratio to the chord is given by

$$r = \frac{(0.2969)^2}{0.8} t^2$$

$$= 1.10\, t^2$$

The ordinates of the six basic sections having thickness-to-chord ratios 0.06, 0.09, 0.12, 0.15, 0.18, and 0.21 are given in Table I.

The airfoil models are made of heat-treated duralumin. A special airfoil generating machine is employed that works from a six-fold templet of the section. The templets are carefully laid out on a layout table that permits the plotting of the stations and ordinates to an accuracy of 0.001 inch. The templets are then cut out and checked for precision of contour. A section of the model airfoil is also checked after the cut is started and any necessary corrections are made on the templet. As the cut progresses, the maximum thickness is checked from time to time to guard against errors resulting from excessive tool wear.

The models are hand-finished to remove small tool marks and then buffed to produce a polished surface. To insure accuracy of alignment in the tunnel, a special drilling jig is employed to drill the airfoil models for mounting.

TESTS

The tests were conducted in the redesigned variable density tunnel. A report describing the tunnel and the details of airfoil testing is being prepared but, because this report is not yet available and because the tunnel has been modified in several important respects since a description of it has been published, a short description of the tunnel and of the details of the tests will be included here. Several changes will be noted if the diagrammatic section of the tunnel shown in Figure 2 is compared with previously published ones. (See references 2 and 3.) As a result of these changes the air flow in the tunnel has been improved. The variation of the air-flow direction, as indicated by a yaw head when passed across the test section, is less than $\pm 1/4^{\circ}$. The velocity distribution at the test section is also very satisfactory. Aside from a small central region, approximately 3 inches in diameter, in which the velocity is less than 1 per cent low, the dynamic pressure is approximately uniform across the test section.

The models are mounted in the tunnel by means of pins at the upper ends of the two main supporting struts shown in Figure 2. The pins are located, with reference to the model, on the chord line one-quarter of the chord behind the leading edge; and with reference to the balance, in line with the intersection of the drag and lift balance linkages. (See fig. 2.) The location of the pins with respect to the balance is checked from time to time and changed, if necessary, so that loads applied to the pins produce no deflection of the moment balance. The accuracy of the moment balance has also been increased, so that accurate moment values measured about the quarter chord point may be obtained directly from the balance.

The airfoil tests were made at only one value of the Reynolds Number, approximately 3,000,000. This value was obtained by using an air pressure in the tunnel of approx-

imately 20 atmospheres (the highest at which the tunnel is usually operated), and by using a slightly reduced speed to maintain the dynamic pressure at such a value that the counters, which read the balance loads, indicated directly the values of the coefficients. It was thus possible to plot the final curves of the coefficients as the test progressed. The Reynolds Number of 3,000,000 corresponds approximately to that reached by most airplanes in flight near minimum speed. The method of testing was otherwise nearly the same as that described in reference 3.

The tare drag was determined by measuring the drag of the supporting members while they were connected inside a hollow dummy airfoil mounted independently of the balance. These measurements were made with the dummy airfoil at several angles of attack. The tare drag at zero angle, expressed as a coefficient based on the wing area, was found to be 0.0055.

The zero angle attitude of the airfoil and the drag coefficients were corrected for air flow misalignment. A slight upflow in the neighborhood of the airfoil results from the damming effect of the support struts and support-strut fairings. The effective value of the upflow angle, as determined from tests of airfoils in erect and inverted positions, is 0.0050 radian. One-half of one per cent of the lift is therefore added to the drag and the zero angle is set slightly below the horizontal. The alignment of the balance with the horizontal is checked from time to time by noting the drag balance deflection as weights are placed on the main balance frame.

RESULTS

The results are presented in tabular and in graphic form. The lift coefficient, angle of attack, drag coefficient and moment coefficient are given in Tables II to VII. The lift coefficient C_L is considered as the independent variable. The lift coefficient values as measured in the tunnel are therefore given in the tables. The angle of attack α_o is the angle of attack corrected to infinite aspect ratio by the method described in reference 1. The angle of attack for aspect ratio 6 may be obtained by adding 3.58 C_L degrees. The drag coefficient C_{D_o} is the

profile drag coefficient obtained from the test data by deducting the induced drag coefficient calculated by the method described in reference 1. The drag coefficient for aspect ratio 6 may be found by adding 0.0559 C_L^2. The moment coefficient $C_{M_{c/4}}$ is the coefficient of the pitching moment about the quarter chord point and may be considered as independent of aspect ratio.

The profile drag coefficients for all the sections are plotted against the lift coefficient in Figure 3. The lift coefficient curves for all the airfoils are plotted in Figure 4.

DISCUSSION

Variation of the Aerodynamic Characteristics with Thickness

The minimum drag coefficients for the airfoils are plotted against thickness in Figure 5. It will be noted that the minimum drag coefficient increases progressively with thickness. The minimum profile drag coefficient C_{D_o} minimum may be represented as a function of the thickness by

$$C_{D_o} \text{ min.} = 0.0065 + 0.0083t + 0.097t^2$$

where t is the maximum thickness expressed as a fraction of the chord. The above function is represented as the curve in Figure 5. The points on the same figure are minimum profile drag values taken from the faired profile drag curves.

It is of interest to consider the minimum drag coefficients based on projected frontal area. This type of coefficient, which is employed when the sections are used as strut sections, may be designated C_D'. By dividing the above expression by t,

$$C_D' = \frac{0.0065}{t} + 0.0083 + 0.0972t$$

$$\frac{dC_{D'}}{dt} = -\frac{0.0065}{t^2} + 0.0972$$

and equating to zero,

$$t = 0.258$$

$$C_{D'} \text{ min.} = .0586$$

In other words, the coefficient based on frontal area decreases with increasing thickness throughout the thickness range investigated, and would apparently continue to decrease until a thickness of about 26 per cent was reached.

The variation of the maximum lift coefficient with thickness is indicated in the following table:

Airfoil	$C_L$max.
0006	0.867
0009	1.195
0012	1.413
0015	1.412
0018	1.429
0021	1.276

It will be noted that the highest maximum lift coefficients are obtained with the moderately thick airfoils. It should be noted, however, that the lift curves (fig. 4) which have very high maximum values have also comparatively sharp peaks so that in practice the highest maximum lift coefficients may be of little or no value. Subsequent tests of the 0012 airfoil have indicated that the flow is so critical in the region of maximum lift that the results are difficult to reproduce. The estimated uncertainty of the values given for the maximum lifts may be as large as 5 per cent for the airfoils having lift curves that indicate an abrupt break beyond the maximum.

The lift-curve slope changes with thickness as shown in Figure 6. The points on the figure represent the deduced slopes for an infinite span wing. It will be noted that all of the values lie below the theoretical value for thin wings, 2π per radian. These results are in ac-

cord with previous results (reference 1) in that the lift-curve slope tends to decrease with increasing thickness.

The moment coefficient for zero angle of attack would be zero for all the airfoils if the flow and the airfoils were exactly symmetrical. Thin-airfoil theory indicates that the pitching moment about a point one-quarter of the chord behind the leading edge is zero. Actually, these results indicate that the pitching moment is very nearly zero at zero angle, but that the moment about the quarter chord point, instead of remaining zero, increases with the angle of attack, as shown in Figure 7, until the angle of attack approaches that of maximum lift. The departure from the theory increases with increasing thickness. This subject will be discussed further under the heading, "Variation of Characteristics with Lift or Angle."

The general efficiency of an airfoil can not be indicated by means of a single number. The ratio of the maximum lift to minimum profile drag is, however, of some value as a measure of the efficiency of an airfoil section. This ratio is largest for the sections between 9 and 12 per cent thick and falls off rapidly when the thickness is increased beyond 18 per cent. The variation of this ratio with thickness is indicated in Figure 8.

Variation of Characteristics with Lift or Angle

The variation of the profile drag coefficient with lift coefficient for all the sections is shown in Figure 3. In reference 4 the variation of the profile drag coefficient with lift coefficient was approximately represented by a single function of the lift coefficient for all airfoils. It is evident, however, that the present results, which are more accurate and cover a greater range of thickness, do not indicate the same variation of the drag with lift for the different airfoils.

If the increase of the profile drag coefficient with lift coefficient could be approximately represented as being proportional to the square of the lift coefficient, then, following the method developed for performance prediction at California Institute of Technology, the additional profile drag could be included with the induced drag. The additional profile drag coefficients

$C_{D_o} - C_{D_o}$ min. are plotted against the square of the lift coefficient in Figure 9. The straight line

$$C_{D_o} - C_{D_o} \text{ min.} = 0.0062C_L^2$$

represents the additional profile drag coefficient of the 0012, 0015, and 0018 airfoils for any lift coefficient between 0 and 1 to a precision of ± 6 per cent of the minimum drag of the 0015. Combining the above equation with the empirical equation previously developed to represent the variation of the minimum profile drag coefficient with thickness, the following equation is obtained. It represents the profile drag coefficient of the moderately thick N.A.C.A. symmetrical airfoils at values of the lift coefficient below 1

$$C_{D_o} = 0.0065 + 0.0083t + 0.0972t^2 + 0.0062C_L^2$$

It is of interest to note that the factor $0.0062C_L^2$ is 11.7 per cent of the induced drag of an elliptical wing of aspect ratio 6.

The fact that the moment coefficients near zero lift increase with increasing lift coefficients (fig. 7) indicates that the center of pressure is ahead of the 25 per cent chord point. The following table indicates the points about which the moment coefficients are constant. In other words, the airfoils are stable in pitch for moderate angles of pitch about axes ahead of this point and unstable about axes behind the point.

Airfoil	Distance from 1/4 chord point forward to point of zero moment (per cent of chord)
N.A.C.A. 0006	0.8
N.A.C.A. 0009	.7
N.A.C.A. 0012	1.2
N.A.C.A. 0015	1.4
N.A.C.A. 0018	1.7
N.A.C.A. 0021	2.1

The centers of pressure for small angles of attack are shown to be farther forward for the thick airfoils. The differences, however, are small and are so influenced by tip effects that the equilibrium points indicated in the table may not be taken as accurately representing properties of the sections.

CONCLUSIONS

These results show that the aerodynamic characteristics of related symmetrical airfoils vary systematically with the thickness ratio of the section. The highest value of the ratio of maximum lift to minimum drag was found to correspond with a thickness ratio of a little less than 0.12.

Langley Memorial Aeronautical Laboratory,
National Advisory Committee for Aeronautics,
Langley Field, Va., July 15, 1931.

REFERENCES

1. Jacobs, Eastman N., and Anderson, R. F.: Large-Scale Aerodynamic Characteristics of Airfoils as Tested in the Variable Density Wind Tunnel. N.A.C.A. Technical Report No. 352, 1930.

2. Jacobs, Eastman N.: The Aerodynamic Characteristics of Eight Very Thick Airfoils in the Variable Density Wind Tunnel. N.A.C.A. Technical Report No. 391, 1931.

3. Munk, Max M., and Miller, Elton W.: The Variable Density Wind Tunnel of the National Advisory Committee for Aeronautics. N.A.C.A. Technical Report No. 227, 1926.

4. Higgins, George J.: The Prediction of Airfoil Characteristics. N.A.C.A. Technical Report No. 312, 1929.

TABLE I

Ordinates of N.A.C.A. Airfoils

Station	Ordinates (% chord)						
% chord	basic	0006	0009	0012	0015	0018	0021
0	0	0	0	0	0	0	0
1.25	3.1565	.947	1.420	1.894	2.367	2.841	3.314
2.5	4.3579	1.307	1.961	2.615	3.268	3.922	4.576
5.0	5.9245	1.777	2.666	3.555	4.443	5.332	6.221
7.5	6.9998	2.100	3.150	4.200	5.250	6.300	7.350
10.0	7.8046	2.341	3.512	4.683	5.853	7.024	8.195
15	8.9086	2.673	4.009	5.345	6.681	8.018	9.354
20	9.5626	2.869	4.303	5.738	7.172	8.606	10.041
30	10.0029	3.001	4.501	6.002	7.502	9.003	10.503
40	9.6717	2.902	4.352	5.803	7.254	8.705	10.155
50	8.8234	2.647	3.971	5.294	6.618	7.941	9.265
60	7.6056	2.282	3.423	4.563	5.704	6.845	7.986
70	6.1065	1.832	2.748	3.664	4.580	5.496	6.412
80	4.3719	1.312	1.967	2.623	3.279	3.935	4.590
90	2.4128	.724	1.086	1.448	1.810	2.172	2.533
95	1.3443	.403	.605	.807	1.008	1.210	1.412
100	.2100	.063	.095	.126	.158	.189	.221
L.E.Rad.	4.405	.394	.887	1.576	2.464	3.549	4.830

TABLE II

Airfoil: N.A.C.A. 0006

Average Reynolds Number: 3,120,000.
Size of model: 5 X 30 inches.
Pressure, standard atmospheres: 20.8.
Test No.: 555. Variable Density Tunnel.
Date: April 8, 1931.

C_L	α_o	C_{D_o}	$C_{M_{c/4}}$
-0.847	-11.3	0.1582	0.055
-.786	-9.5	.1324	.020
-.613	-6.0	.0129	-.005
-.311	-3.0	.0078	-.003
.004	0	.0070	0
.157	1.5	.0077	.002
.315	3.0	.0084	.003
.620	6.0	.0135	.004
.794	9.5	.1195	-.025
.848	11.3	.1645	-.059
.867	13.2	.2125	-.090
.857	15.3	.2528	-.110
.835	17.3	.2877	-.125
.823	21.4	.3588	-.135
.819	27.4	.4695	-.145

TABLE III

Airfoil: N.A.C.A. 0009

Average Reynolds Number: 3,110,000.
Size of model: 5 × 30 inches.
Pressure, standard atmospheres: 20.6
Test No.: 558. Variable Density Tunnel.
Date: April 9, 1931.

C_L	α_o	C_{D_o}	$C_{M_{c/4}}$
-1.048	-10.7	0.0175	-0.005
-.905	-9.1	.0137	-.003
-.602	-6.1	.0101	-.004
-.298	-3.1	.0083	-.002
.011	0	.0080	.001
.165	1.5	.0082	.003
.316	3.0	.0088	.001
.622	6.0	.0104	.004
.915	9.1	.0144	.003
1.064	10.6	.0170	0
1.195	12.2	.0312	-.001
1.099	14.5	.1383	-.049
1.037	16.7	.2255	-.085
.909	21.1	.3417	-.121
.813	27.4	.4614	-.138

TABLE IV

Airfoil: N.A.C.A. 0012

Average Reynolds Number: 3,230,000.
Size of model: 5 × 30 inches.
Pressure, standard atmospheres: 20.4.
Test No.: 562. Variable Density Tunnel.
Date: April 13, 1931.

C_L	α_o	C_{D_o}	$C_{M_{c/4}}$
-1.187	-12.2	0.0194	-0.002
-.904	-9.1	.0137	-.003
-.604	-6.1	.0108	-.005
-.289	-3.0	.0090	-.002
.003	0	.0089	-.001
.155	1.5	.0090	.001
.310	3.0	.0096	.002
.610	6.1	.0111	.008
.912	9.1	.0141	.011
1.195	12.2	.0207	.008
1.325	13.8	.0252	.003
1.413	15.2	.0337	.003
1.160	16.9	.1562	-.054
.990	20.9	.2811	-.096
.864	27.3	.4295	-.128

TABLE V

Airfoil: N.A.C.A. 0015

Average Reynolds Number: 3,110,000.
Size of model: 5 X 30 inches.
Pressure, standard atmospheres: 20.4.
Test No.: 560. Variable Density Tunnel.
Date: April 10, 1931.

C_L	α_o	C_{D_o}	$C_{M_{c/4}}$
-1.195	-12.2	0.0204	-0.002
-.915	-9.1	.0145	-.001
-.611	-6.1	.0119	--
-.312	-3.0	.0102	-.001
-.009	0	.0099	.003
.144	1.5	.0100	.003
.294	3.1	.0106	.007
.600	6.1	.0117	.009
.895	9.2	.0143	.009
1.176	12.3	.0198	.010
1.304	13.9	.0245	.011
1.407	15.5	.0336	.003
1.412	15.6	--	--
1.228	17.1	--	--
1.191	18.2	.1605	-.040
1.134	20.4	.2149	-.066
.876	27.2	.3834	-.109

TABLE VI

Airfoil: N.A.C.A. 0018

Average Reynolds Number: 3,140,000.
Size of model: 5 X 30 inches.
Pressure, standard atmospheres: 20.8
Test No.: 553. Variable Density Tunnel.
Date: April 7, 1931.

C_L	α_o	C_{D_o}	$C_{M_{c/4}}$
-.896	-9.3	0.0156	-0.011
-.603	-6.1	.0130	-.011
-.305	-3.0	.0113	-.006
-.006	0	.0110	.002
.144	1.5	.0109	.002
.294	3.1	.0115	.005
.598	6.1	.0130	.009
.881	9.2	.0156	.007
1.160	12.3	.0205	.009
1.404	15.5	.0322	.012
1.429	16.5	--	--
1.309	17.8	.1107	-.018
1.251	20.0	.1735	-.036
1.023	24.7	.3022	-.082

TABLE VII

Airfoil: N.A.C.A. 0021

Average Reynolds Number: 3,180,000.
Size of model: 5 × 30 inches.
Pressure, standard atmospheres: 20.6.
Test No.: 559. Variable Density Tunnel.
Date: April 10, 1931.

C_L	α_o	C_{D_o}	$C_{M_{c/4}}$
-1.123	-12.4	0.0255	-0.013
-.863	-9.3	.0184	-.013
-.575	-6.2	.0154	-.010
-.288	-3.1	.0134	-.005
-.004	0	.0124	.001
.142	1.5	.0130	.004
.284	3.1	.0133	.007
.574	6.2	.0146	.012
.854	9.3	.0176	.015
1.120	12.4	.0249	.016
1.224	14.1	.0330	.015
1.276	14.9	.0409	.010
1.229	16.1	.0792	-.004
1.144	20.4	.1863	-.035
.996	26.8	.3061	-.079

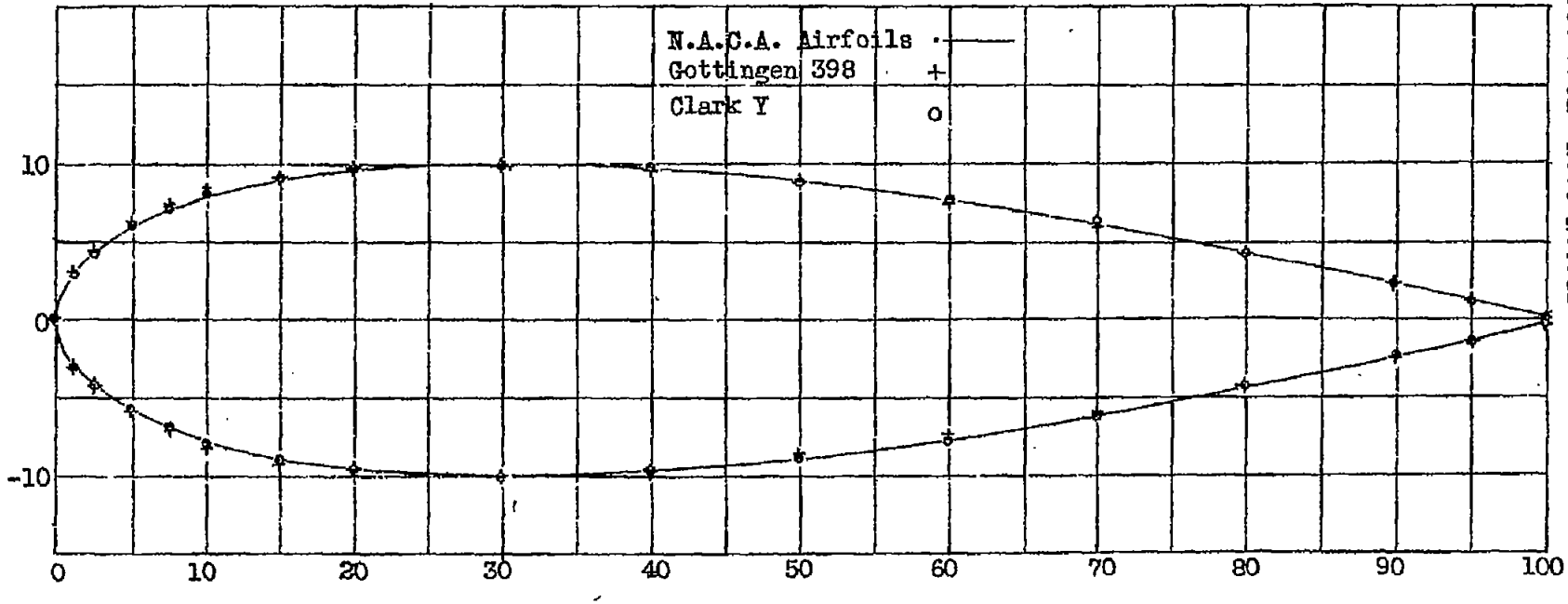

Fig.1 Thickness variation.

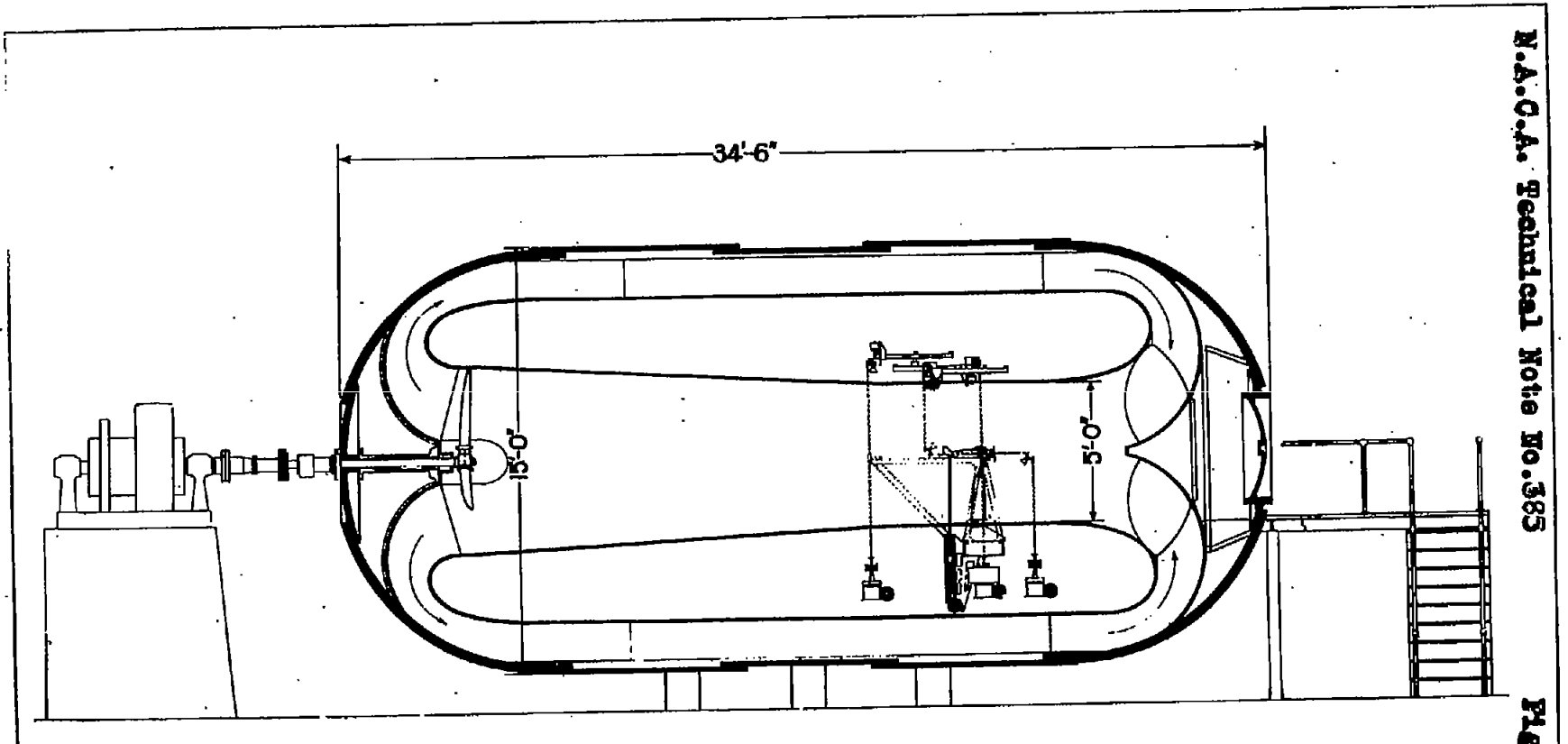

Fig.2 Diagrammatic section of the redesigned Variable Density Wind Tunnel.

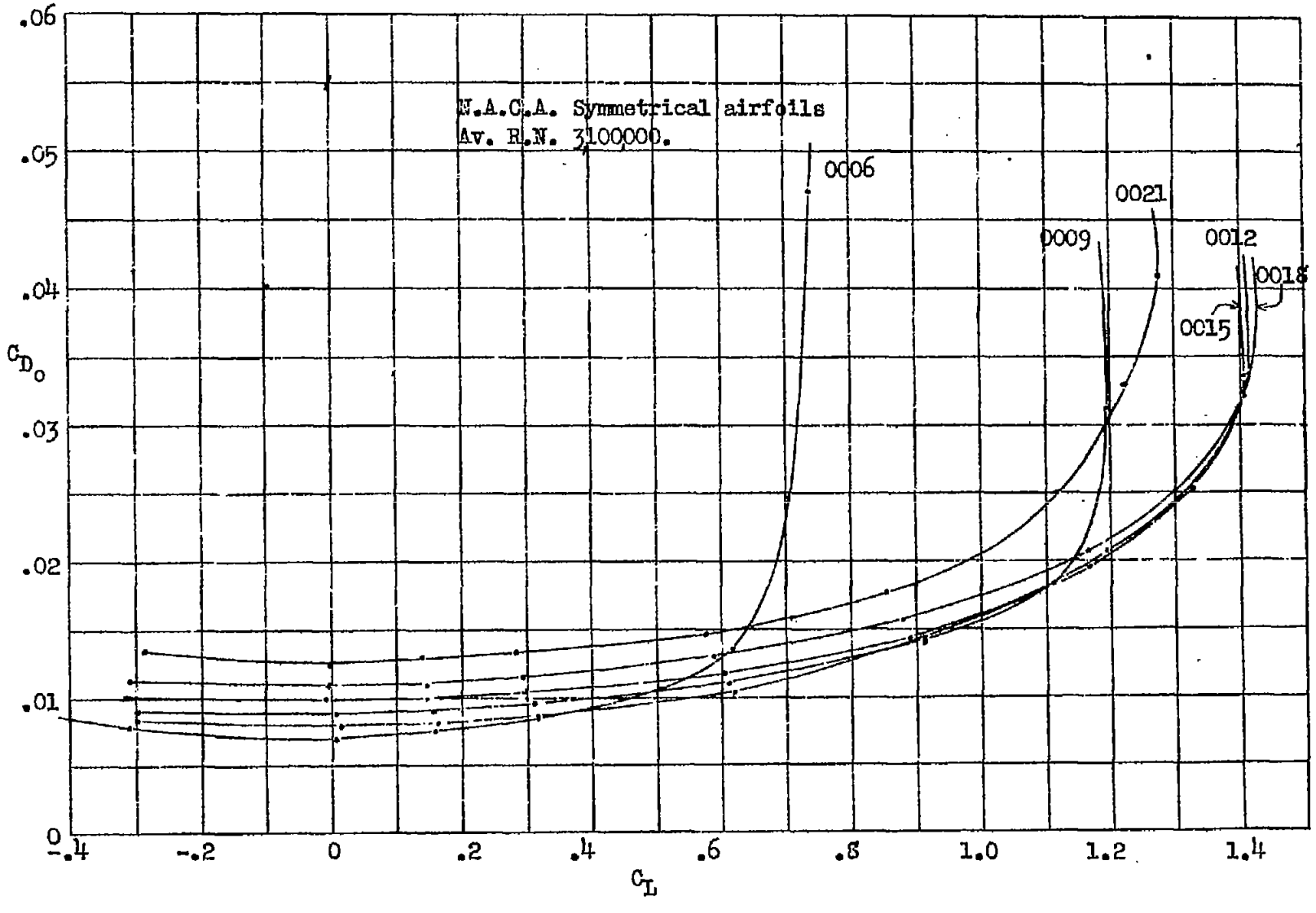

Fig.3 Profile drag curves.

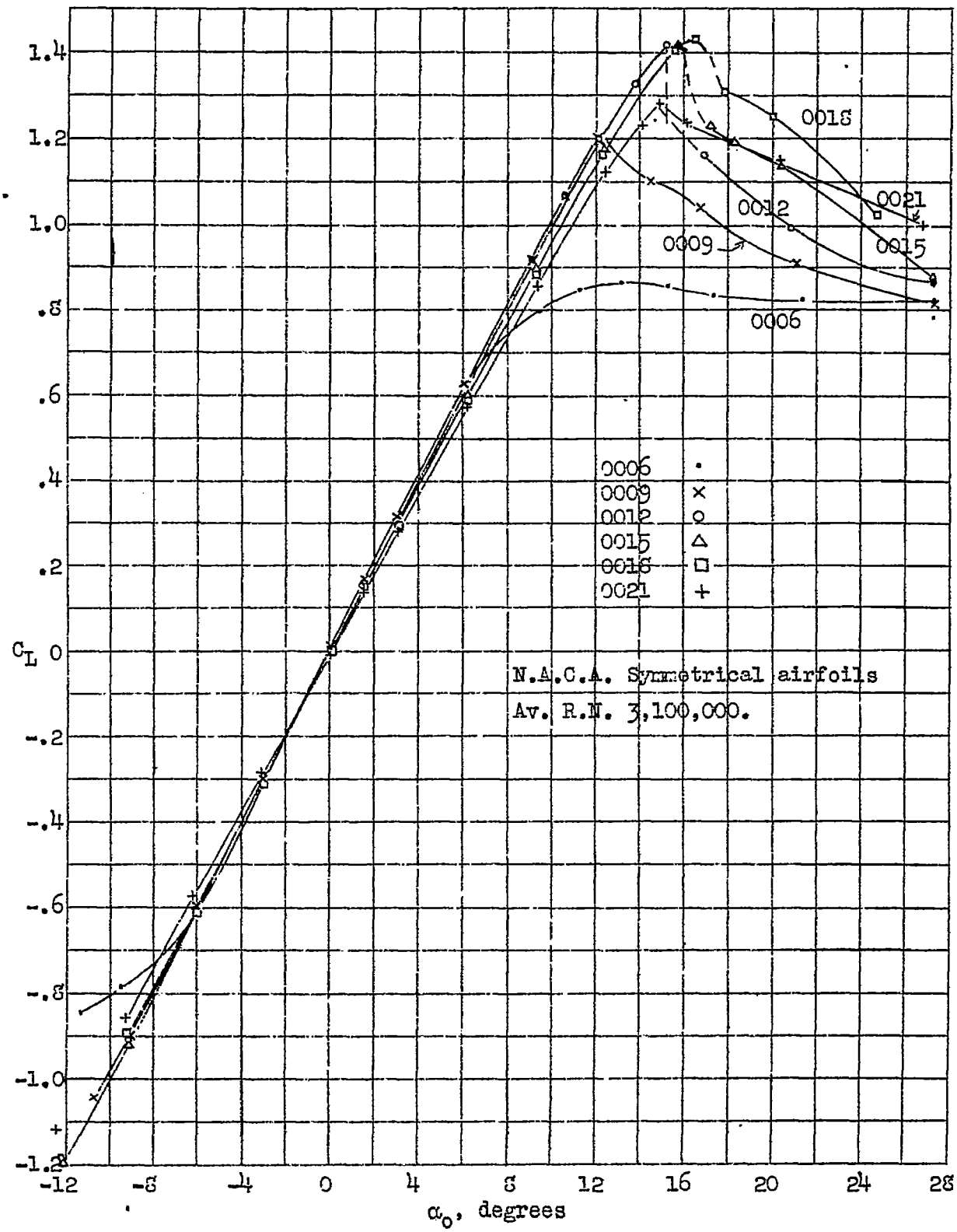

Fig.4 Lift curves corrected to infinite aspect ratio.

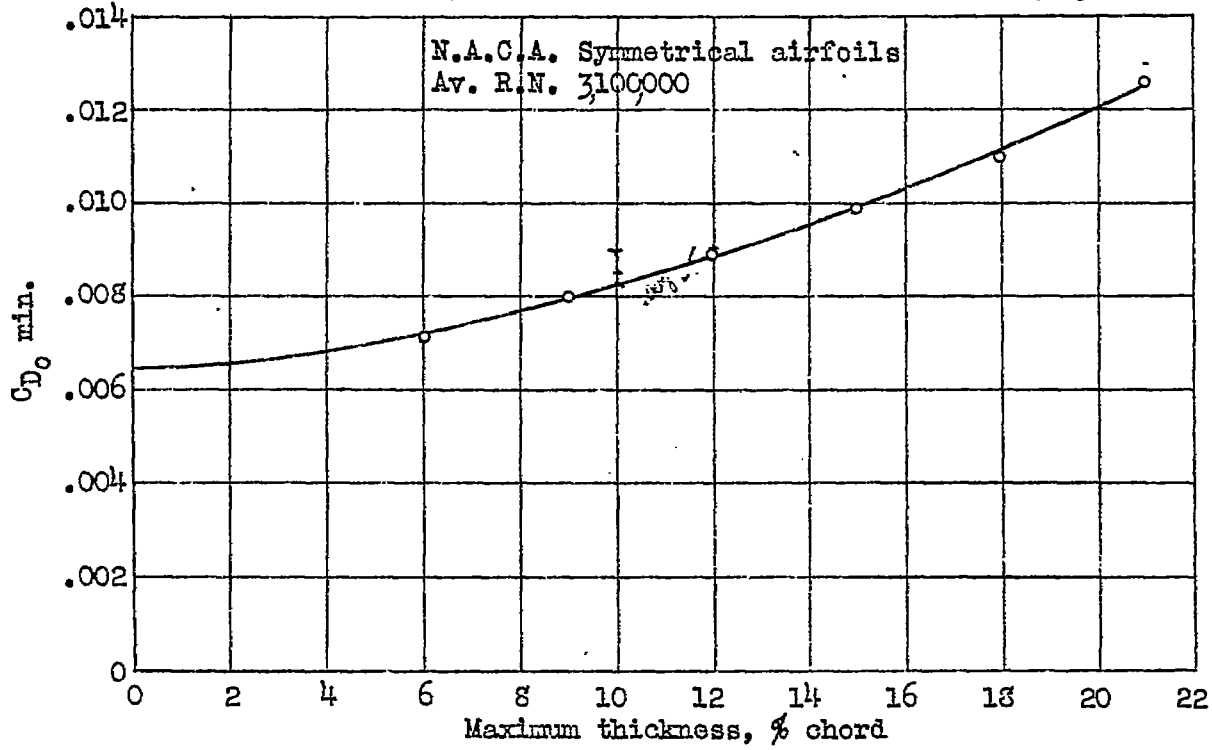

Fig.5 Variation of minimum profile drag with thickness.

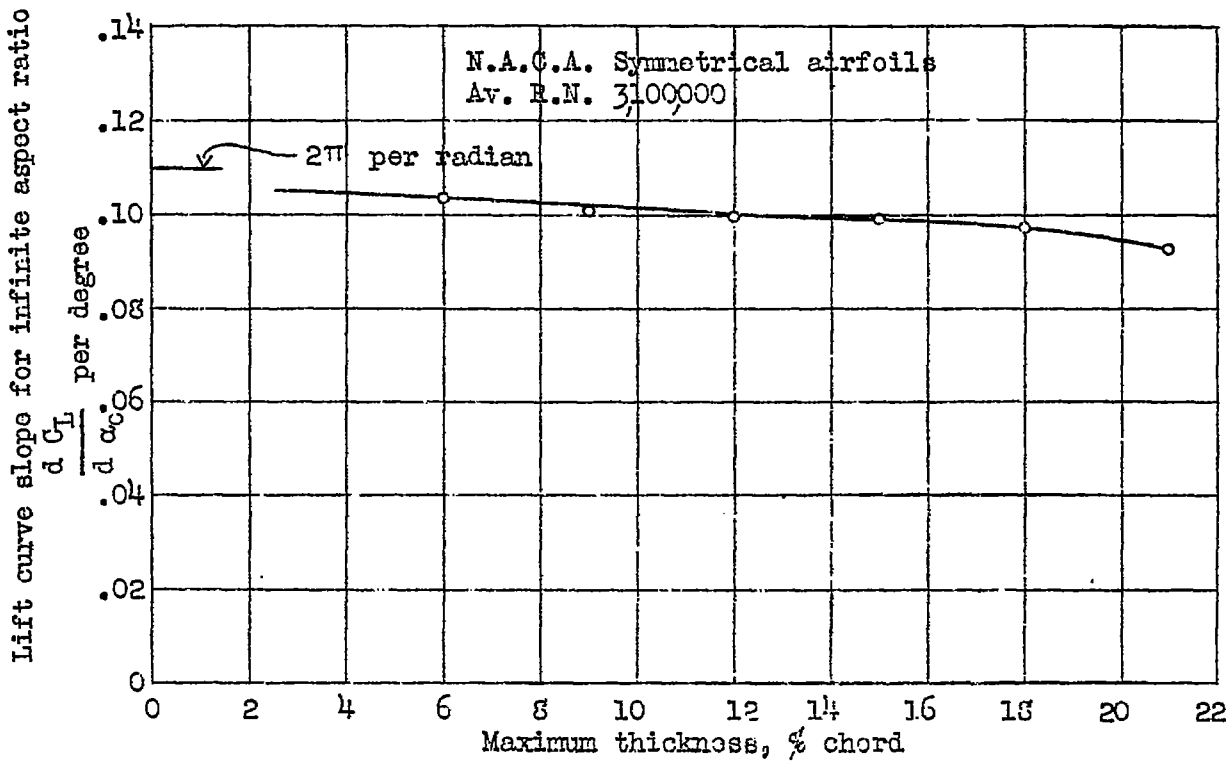

Fig.6 Variation of lift-curve slope with thickness.

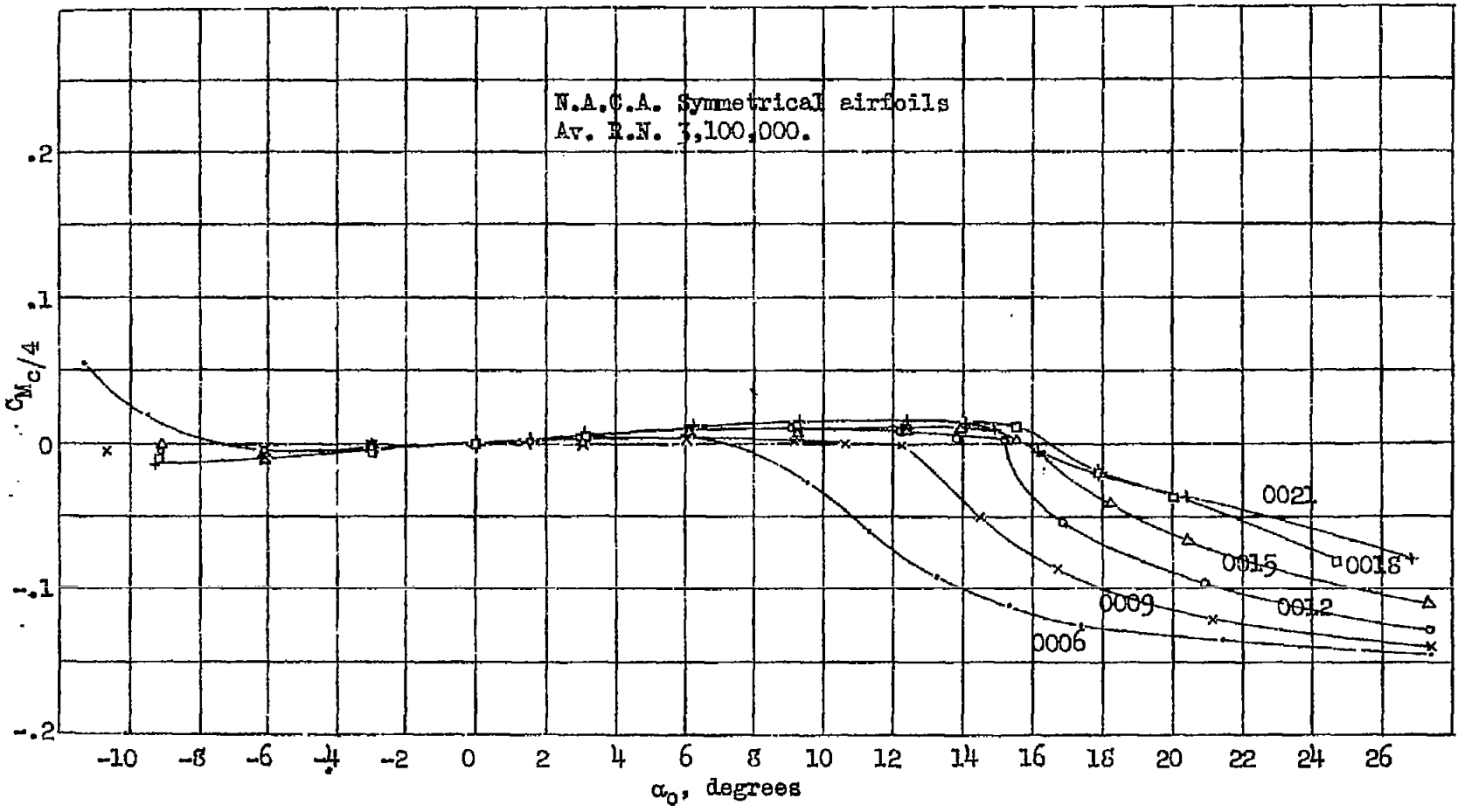

Fig.7 Moment coefficients.

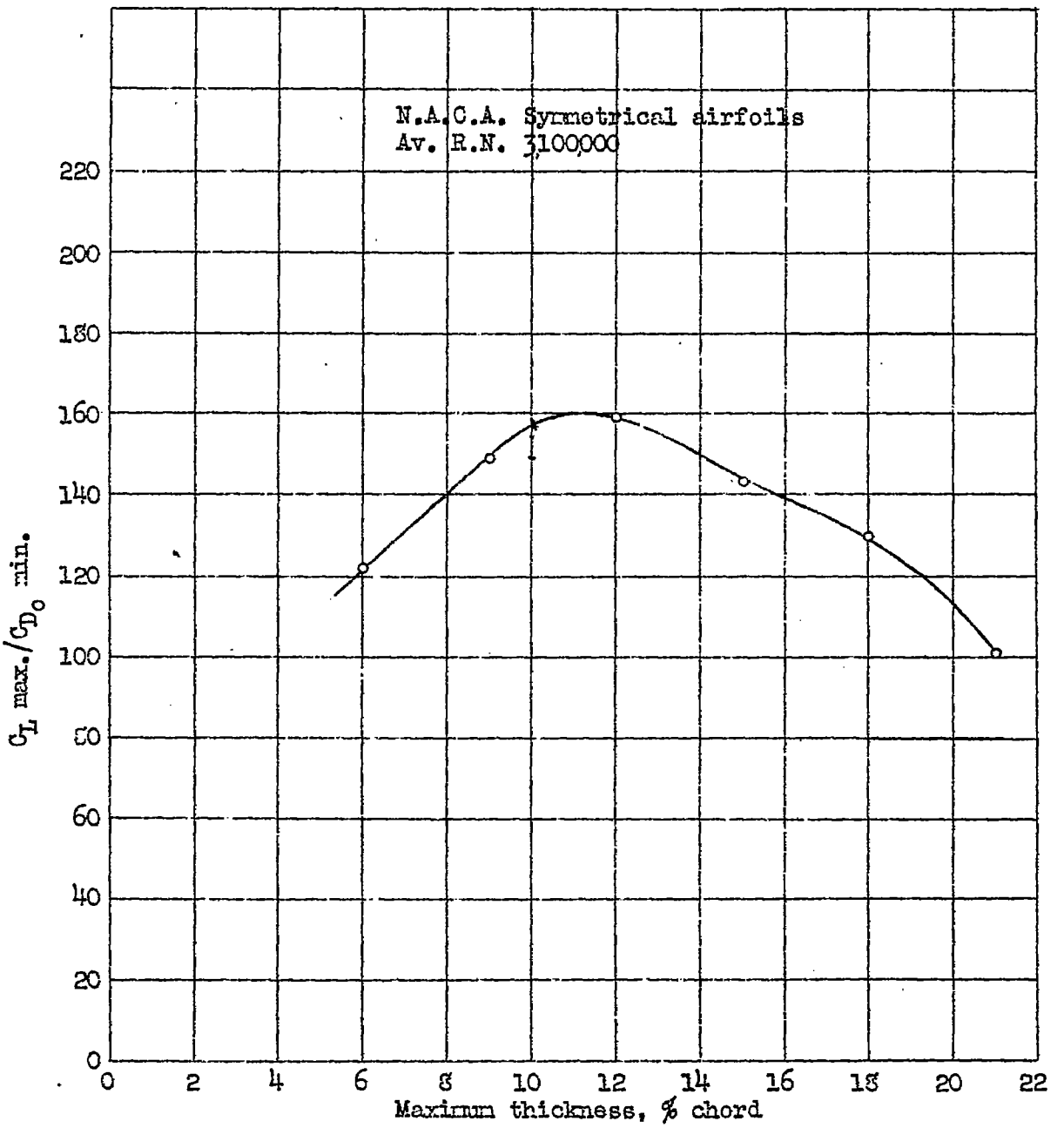

Fig.8 Ratio of maximum lift to minimum profile drag.

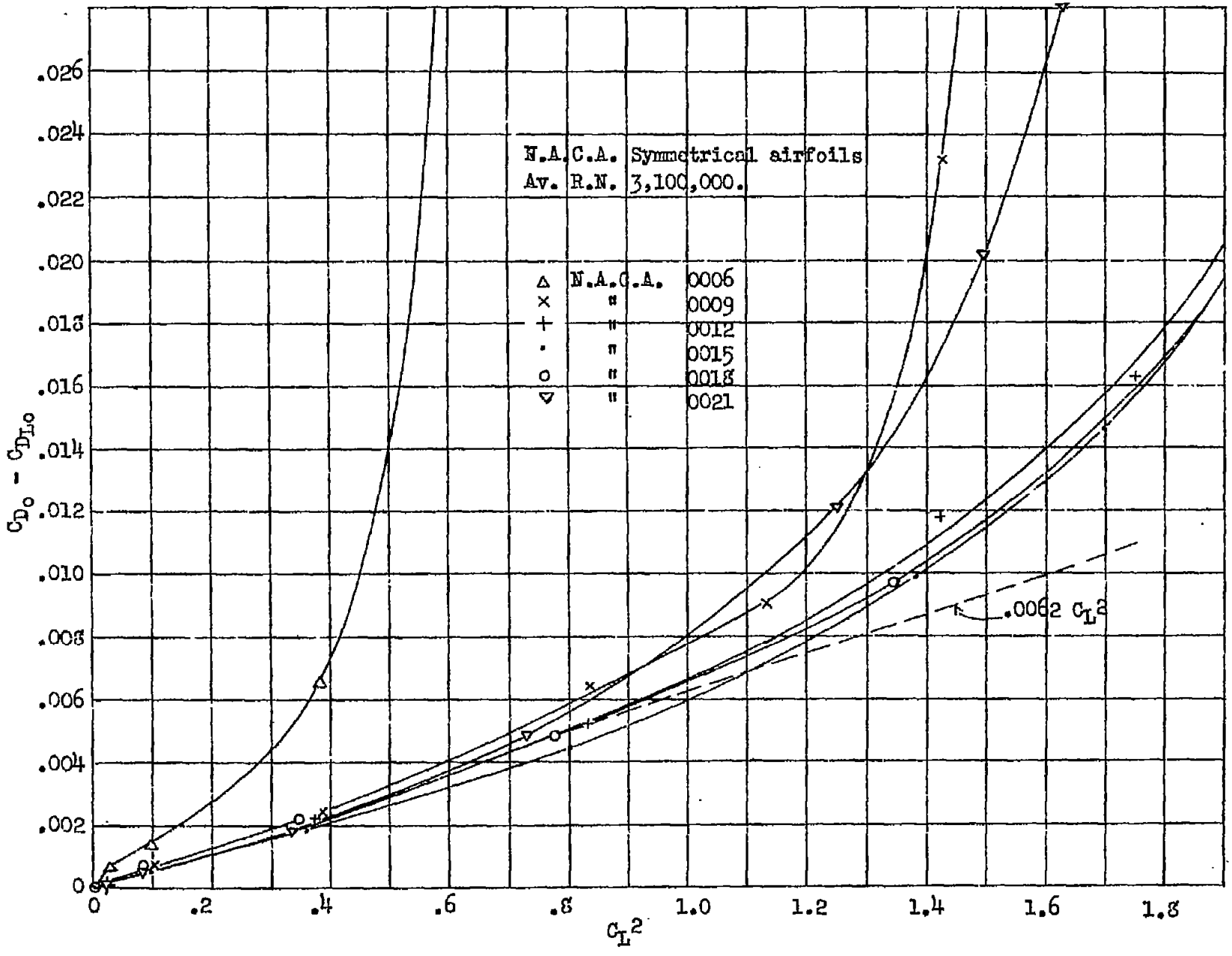

Fig.9 Increase of profile drag with lift coefficient.